

Model for optical absorption in porous silicon

Shouvik Datta* and K. L. Narasimhan

Solid State Electronics Group, Tata Institute of Fundamental Research, Homi Bhabha Road, Colaba, Mumbai 400 005, India

(Received 22 February 1999)

In this paper we analyze the optical absorption in porous silicon. This is the first attempt to explicitly demonstrate that it is not possible to extract the band gap of low-dimensional nanostructures like porous silicon from a Tauc plot of $\sqrt{\alpha\hbar\omega}$ vs $\hbar\omega$. So we model the absorption process assuming that porous silicon is a pseudo-one-dimensional material system having a distribution of band gaps. We show that in order to explain the absorption we specifically need to invoke the following: (a) k is not conserved in optical transitions, (b) the oscillator strength of these transitions depends on the size of the nanostructure in which absorption takes place, and (c) the distribution of band gaps significantly influences the optical absorption. A natural explanation of the temperature dependence of absorption in porous silicon also follows from our model.

[S0163-1829(99)03435-9]

I. INTRODUCTION

The discovery of efficient photoluminescence^{1,2} from porous silicon (PS) has attracted the attention of many researchers. The photoluminescence peak occurs at an energy greater than the band gap of *c*-silicon and can be tuned through the visible spectrum by changing the preparation conditions. Canham,¹ proposed that PS is a nanostructured material and the band gap of these nanostructures is enhanced due to quantum size effects. He argued that this would account for the fact that the luminescence energy is greater than the band gap of *c*-silicon. Evidence for the increase in the band gap was first reported by Lehmann—from optical-absorption measurements.³ Transmission electron microscopy measurements reveal that the diameter of the columnar nanostructures that make up PS depends on preparation conditions and can be as small as 2–4 nm.^{2,3} PS can hence be thought of as an assembly of pseudo-one-dimensional (1D) quantum wires. The progress in this area has been the subject of many recent reviews.^{4–8} In this paper we confine ourselves to the understanding of the optical-absorption process in PS.

There have been many attempts to obtain the band gap of PS from optical-absorption measurements.^{9–13} In these measurements the authors assume that the absorption coefficient (α) of PS satisfies the same relation as in three-dimensional (3D) bulk *c*-silicon, viz.,

$$\sqrt{\alpha\hbar\omega} = D(\hbar\omega - E_g). \quad (1)$$

The Tauc plot ($\sqrt{\alpha\hbar\omega}$ vs $\hbar\omega$) is a straight line and the intercept on the energy axis gives the band gap E_g . The use of this equation for a one-dimensional system like PS suffers from the following criticisms.

(1) In general, the absorption coefficient depends on the joint density of states (JDOS) of the material. Equation (1) is valid only when the density of states $g(E)$ varies¹⁴ with energy near the band edges as $g(E) = M\sqrt{E}$, where E is measured from the band edge and M is a constant. If we treat PS as a 1D material (up to a first approximation assuming parabolic band structure) it would be more appropriate to write

the density of state $g(E) = N/\sqrt{E}$ (N is a constant) than the common practice of using a 3D density of state. Clearly the JDOS in PS is expected to be different from that of bulk *c*-silicon. For a 1D system having a single direct band gap E_g , it is easy to show that the JDOS is proportional to $N/\sqrt{E-E_g}$. In such a case, a plot of $\alpha(E)$ vs E should peak at E_g . On the other hand, for an indirect band-gap material (assuming that the momentum k is not conserved in this pseudo-1D system in an optical transition), it is easy to show that the JDOS is a constant and independent of incident energy (following Ref. 14). Therefore, in either case, $\sqrt{\alpha\hbar\omega}$ is not linearly related with $\hbar\omega$ at all. Clearly the use of Eq. (1) to extract the band gap is not justified for PS.

(2) The nanostructures that make up PS have a distribution^{2,3,8} of diameters (d). If the band gap is related to quantum size effects, then it is clear that the energy upshift ΔE (which can be written as $\Delta E = C/d^X$) is different for each of the nanostructures that make up PS. (The value of X in the simplest approximation is 2; further details of this are discussed in Sec. III). In PS, we are actually dealing with a heterogeneous system with a distribution of band gaps. Hence it may not be meaningful to visualize PS as having a single band gap and that this can be extracted from Eq. (1).

At this junction, we would also like to point out that the above objections against the common practice of using¹⁵ Eq. (1) to get the band gap are equally valid in case of other low-dimensional systems like quantum dots, etc.

In an attempt to address these questions we have investigated the optical absorption in PS specifically using the 1D density of states. In this paper we clarify the absorption process in PS assuming that it has a distribution of band gaps. Section II contains the experimental results which will be used for comparing our simulations. Here we report a non-destructive way of measuring the porosity of PS thin films using transmission measurements and effective-medium theory. Section III outlines the model used for calculating optical absorption and Sec. IV gives the results of our simulations. On the basis of the simulations we will further consolidate our viewpoint that the Tauc plot cannot be used to determine the band gap of low-dimensional systems. We

also show that we can easily explain the temperature dependence of the absorption in PS using our model. Finally we summarize our conclusions in Sec. V.

II. EXPERIMENTAL RESULTS

We have done some experiments to facilitate the comparison of our simulations with real experimental data. PS is made by electrochemical etching of *p*-type *c*-Si in a 1:1 HF: ethanol solution at a current density between 10–50 mA/cm². Free-standing samples are lifted off the substrate by increasing the current density to >200 mA/cm². The samples are then washed in water to get rid of HF, rinsed in *n*-pentane, and finally air dried on a glass substrate for transmission measurements.

Transmission measurements are carried out using a CVI 240 Digikrom monochromator with a tungsten lamp as a source, silicon detector, and SR 530 lock-in amplifier. For some samples we also use a Cary 1756 spectrometer. We have checked that internal multiple scattering does not dominate the absorption in our samples. This is done by making two PS samples of two different thicknesses (5 and 10 μm, respectively) and ensuring that the transmission curves are the same for both samples at low absorption.¹¹

The absorption coefficient $\alpha(\lambda)$ as a function of wavelength λ is obtained from the normalized transmittance $T(\lambda)$ using¹⁴

$$T(\lambda) = \frac{(1-R)^2 \exp[-\alpha(\lambda)(1-P)t]}{1-R^2 \exp[-2\alpha(\lambda)(1-P)t]}. \quad (2)$$

The reflectivity (R) is obtained in the low α region using the relation $R = (1-T)/(1+T)$. P is the porosity of the layer and t is its thickness.

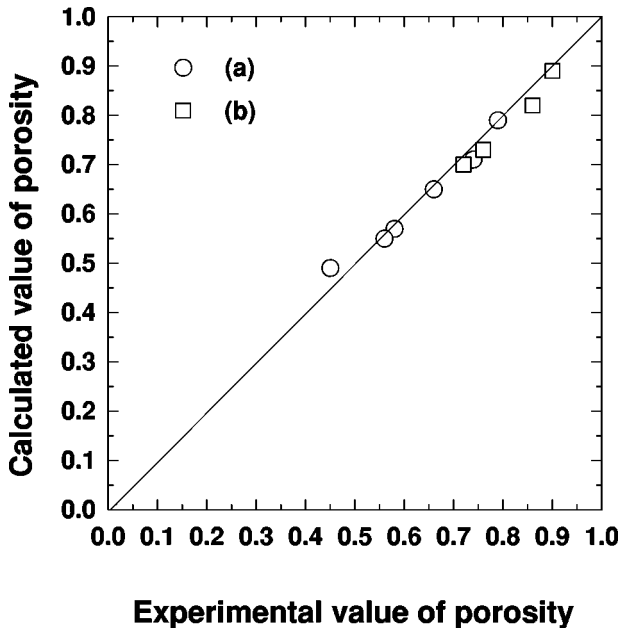


FIG. 1. Porosity calculated [using Eq. (7)] from the transmission curves is plotted against the corresponding gravimetrically determined values of porosity. The points fall nearly on a straight line of slope one. (a) Data from Ref. 9 and (b) data from Ref. 16.

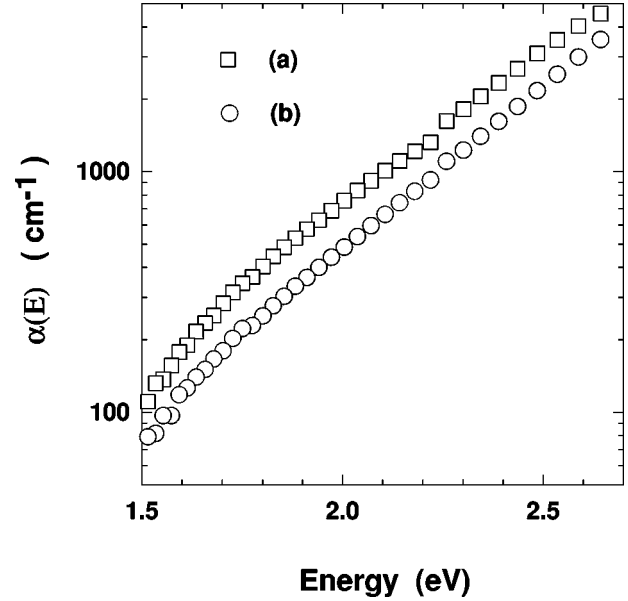


FIG. 2. Temperature dependence of the absorption spectrum of *p*-type porous silicon. (a) 300 K and (b) 100 K.

The porosity of PS is usually determined by gravimetric measurements which destroy the sample. We now show that the optical transmission experiment allows us to measure porosity in a nondestructive fashion.

The normalized transmittance [in Eq. (2)] for $\alpha=0$ reduces to

$$T_L = \frac{(1-R)}{(1+R)} \text{ or } R = \frac{1-T_L}{1+T_L}. \quad (3)$$

If n is the real part of the refractive index, then we can also write for the reflectivity (for $\alpha=0$) as

$$R = \frac{(n-1)^2}{(n+1)^2}. \quad (4)$$

It follows from Eq. (4) that the refractive index (n_{PS}) of PS is

$$n_{PS} = \frac{1+\sqrt{R}}{1-\sqrt{R}}. \quad (5)$$

We model PS as consisting of two media—air [having a refractive index ($n_{air}=1$)] and crystalline silicon ($n_{Si}=3.44$). It was shown earlier¹³ that in the framework of the effective-medium approximation one can write

$$(\epsilon_{PS}-1)/(3\epsilon_{PS}) = (1-P)[(\epsilon_{Si}-1)/(2\epsilon_{PS}+\epsilon_{Si})], \quad (6)$$

where P is the porosity and the dielectric constant $\epsilon=n^2$. Therefore,

$$P = 1 - [(2\epsilon_{PS} + \epsilon_{Si})(\epsilon_{PS} - 1) / (\epsilon_{Si} - 1)(3\epsilon_{PS})]. \quad (7)$$

The porosity can now be obtained using Eqs. (4) to (7).

To check the validity of Eq. (7), we calculate the porosity [using Eq. (7)] and compare it with the corresponding values of P obtained gravimetrically. Figure 1 is a plot of the po-

rosity determined from the transmission curves and the corresponding experimentally determined porosity by gravimetric measurements as reported in the literature.^{9,16} We see from Fig. 1 that the points nearly fit a straight line with slope one. We hence conclude that optical transmission measurements can reliably be used to obtain the porosity of porous silicon in a nondestructive fashion.

Figure 2 is a plot of $\alpha(E)$ vs E at 300 and 100 K. The absorption at low temperature is reduced with respect to that at room temperature. We see that the two curves exhibit a rigid shift in agreement with other results.¹⁰ An explanation of this phenomena on the basis of our simulated results is given in Sec. IV.

We now attempt to understand the optical-absorption process in PS with the help of some model calculations and simulations, assuming that these 1D materials have a distribution of band gaps.

III. A MODEL FOR ABSORPTION IN PS HAVING A DISTRIBUTION OF BAND GAPS

We model the nanostructures that make up PS to be 1D parallelepipeds of square cross sections of side d and constant length L . Since d is typically 20–40 Å, the band gap of the material is enhanced due to quantum size effects. We assume that the effective band gap (lowest energy gap) for a particular parallelepiped is the minimum separation between the conduction-band and the valence-band states for quantum numbers $n_x=1$ and $n_y=1$. We also assume that the absorption takes place in the bulk.

The absorption coefficient $\alpha(E)$ for a particular value of incident energy E can be written as

$$\alpha(E) = \int_{E_G < E} \rho^J(E - E_G) F(E_G) P(E_G) dE_G, \quad (8)$$

where the integration is done over all the band gaps (E_G) of the system below the incident energy E . In Eq. (8), ρ^J is the joint density of states, $F(E_G)$ the oscillator strength for the optical transition, and $P(E_G)$ the distribution of band gaps E_G in the material. We now discuss Eq. (8) in some detail.

We have already pointed out in Sec. I, if $g(E) = N/\sqrt{E}$ then the JDOS (ρ^J) is proportional to $(E - E_G)^{-W}$. The value of W depends on whether PS is a direct or an indirect band-gap material. For direct band-gap material $W=0.5$ and for indirect band gap material $W=0$.

$F(E_G)$ is the oscillator strength governing the absorption. For indirect band-gap material, the oscillator strength¹⁷ can be enhanced for small d . This happens because the overlap between the electron and hole wave functions in k space increases as a result of quantum confinement and contributes to an increase in the oscillator strength at small d (large E_G) and can be written^{18,19} as $F = f/d^\gamma$, where $\gamma=5$ to 6. This manifests itself as the dominant no-phonon line which has been seen recently in the luminescence spectra of PS.²⁰

The third term in Eq. (8), viz., $P(E_G)$, is the distribution of band gaps in PS. The band-gap distribution is obtained by assuming a distribution of sizes for d and a relation governing the upshift in energy ΔE with the size d (due to quantum confinement).

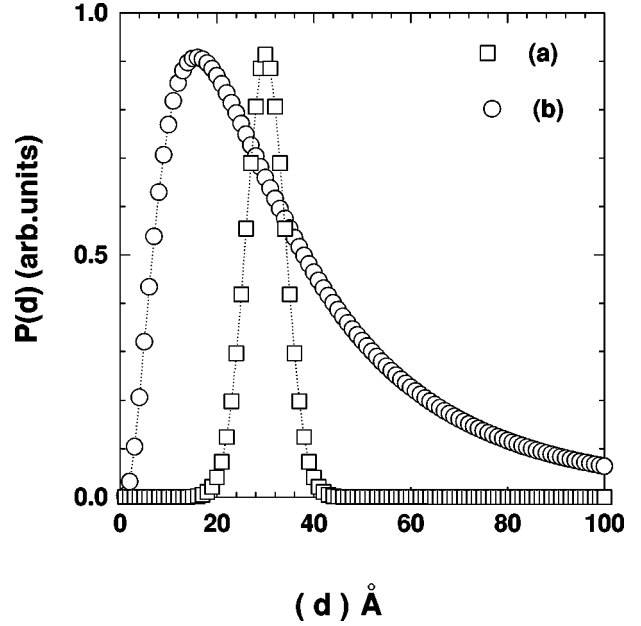


FIG. 3. Size distribution of the column widths (a) for a Gaussian and (b) for a lognormal distribution of widths, having $d_0=30$ Å and $\sigma=4$ Å.

In our model we have considered two possible distribution of sizes. One is Gaussian and the other is lognormal²¹ distribution given by $P^G(d)$ and $P^L(d)$, respectively,

$$P^G(d) = \frac{1}{(\sqrt{2\Pi}\sigma)} \exp\left(-\frac{(d-d_0)^2}{2\sigma^2}\right), \quad (9)$$

where d_0 is the mean size and the σ the standard deviation,

$$P^L(d) = \frac{1}{\sigma_L d \sqrt{2\Pi}} \exp\left(-\frac{[\ln(d) - m_0]^2}{2\sigma_L^2}\right), \quad (10)$$

where $m_0 = \ln(d_0)$, and $\sigma_L = \ln(\sigma)$, d_0 being the mean size and σ the standard deviation.

Electron microscopy measurements^{2,3,22} suggest that for pPS, d_0 is around 30 Å and $\sigma \approx 4$ Å. Figure 3 shows the distribution of sizes for lognormal and Gaussian distributions for $d_0=30$ Å and $\sigma=4$ Å.

The energy up shift for the confinement ΔE can be written as

$$\Delta E = E_G - E_g = C/d^X, \quad (11)$$

where E_g is the crystalline Si fundamental indirect band gap ≈ 1.17 eV and E_G is the increased band gap due to quantum confinement.

The value of X is 2 in the usual effective-mass approximation. However, for nanocrystals, the effective mass itself becomes size dependent and the exponent X has been reported to vary from 1.2–1.8 and becomes 2 at large size.^{17,23} For the purpose of our simulation we consider two cases: (a) $X=2$, $C=486$ eV/Å² ($E_{G0}=1.71$ eV for $d=30$ Å) (Refs. 22 and 24) and (b) $X=1.4$, $C=126$ eV/Å^{1.4} ($E_{G0}=2.25$ eV for $d=30$ Å) (Ref. 23).

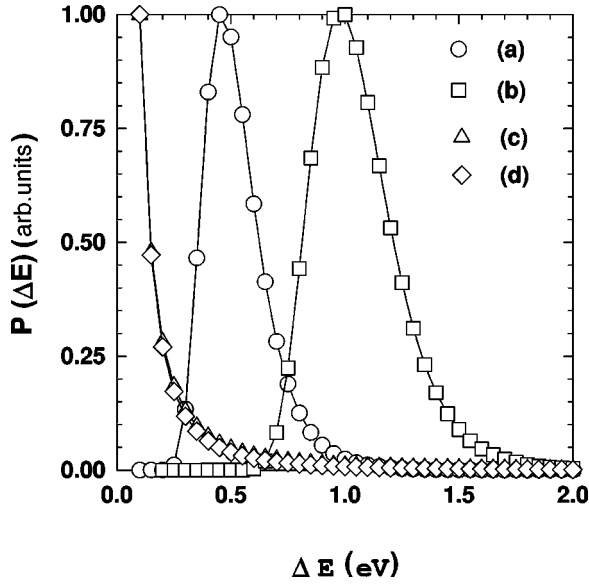


FIG. 4. Band-gap distribution for corresponding size distribution given in (a) and (b) are for Gaussian distribution for $X=2$ and 1.4, respectively. (c) and (d) are for the lognormal distribution for $X=2$ and 1.4, respectively.

The interaction volume of the column structures with incident light is $V(d)=Ld^2$. The resulting distribution $R(d)=P(d)\times V(d)$ is properly normalized to have equal number

of dipole oscillators in each case. We now make a change of variable from d to E_G (using $E_G=E_g+C/d^X$) to get the corresponding distribution $P(E_G)$ of the band gaps.

For a Gaussian distribution of sizes [Eq. (9)]—the distribution of band gaps is

$$P^G(E_G)=P_0(E_G-E_g)^{-(X-3)/X} \times \exp\left\{-A\left[\left(\frac{E_{G0}-E_g}{E_G-E_g}\right)^{1/X}-1\right]^2\right\}, \quad (12)$$

where P_0 is a normalization constant, $A=0.5(d_0/\sigma)^2$, and E_b is the maximum value of E_G .

Following a similar procedure for the lognormal distribution [Eq. (10)] we have

$$P^L(E_G)=R_0(E_G-E_g)^{-(X-2)/X}\sigma_L^{-1} \times \exp\left[-B\left(\frac{\ln(C/E_G-E_g)^{1/X}}{\ln(C/E_{G0}-E_g)^{1/X}}-1\right)^2\right], \quad (13)$$

where R_0 is the normalization constant, $B=0.5(m_0/\sigma_L)^2$.

Figure 4 shows the distribution of band gaps $P(E_G)$ when the energy upshift is given for $X=1.4$ and 2. For the lognormal case, we see that $P(E_G)$ peaks close to the band gap of *c*-si. Equations (8), (12), and (13) are used to calculate $\alpha(E)$ for each incident energy $E=\hbar\omega$.

$\alpha(E)$ for a Gaussian distribution of sizes is given by

$$\alpha^G(E)=\alpha_0\int_0^{E_b}(E-E_G)^{-W}(E_G-E_g)^{(\gamma-X-3)/X}\exp\left\{-A\left[\left(\frac{E_{G0}-E_g}{E_G-E_g}\right)^{1/X}-1\right]^2\right\}dE_G, \quad (14)$$

where α_0 is a normalization constant.

For a lognormal distribution of sizes $\alpha(E)$ is

$$\alpha^L(E)=\beta_0\int_0^{E_b}(E-E_G)^{-W}(E_G-E_g)^{[(\gamma-X-2)/X]}\sigma_L^{-1}\exp\left[-B\left(\frac{\ln(C/E_G-E_g)^{1/X}}{\ln(C/E_{G0}-E_g)^{1/X}}-1\right)^2\right]dE_G, \quad (15)$$

where β_0 is a normalization constant. Equations (14) and (15) are used to simulate various possible absorption processes.

IV. RESULTS OF THE SIMULATION

In this section we present the results for the absorption coefficient as a function of energy for different cases on the

basis of the above model. The values of various exponents for different physical situations are summarized in Table I.

A. Direct band gap

Figure 5 shows $\alpha(\hbar\omega)$ vs $\hbar\omega$ for a direct band gap material where k is conserved in the optical transition and no size dependence of the oscillator strengths ($\gamma=0$) is considered

TABLE I. We have considered these physical situations in the model for the optical absorption in porous silicon for direct transitions $W=0.5$ and indirect transitions $W=0$. The value of γ is taken as 6.0 for size-dependent oscillator strengths and zero for the size-independent case.

Gaussian distribution in d			Lognormal distribution in d		
Case	Value of X	Nature of transition	Case	Value of X	Nature of transition
1	2.0	Direct	5	2.0	Direct
2	2.0	Indirect	6	2.0	Indirect
3	1.4	Direct	7	1.4	Direct
4	1.4	Indirect	8	1.4	Indirect

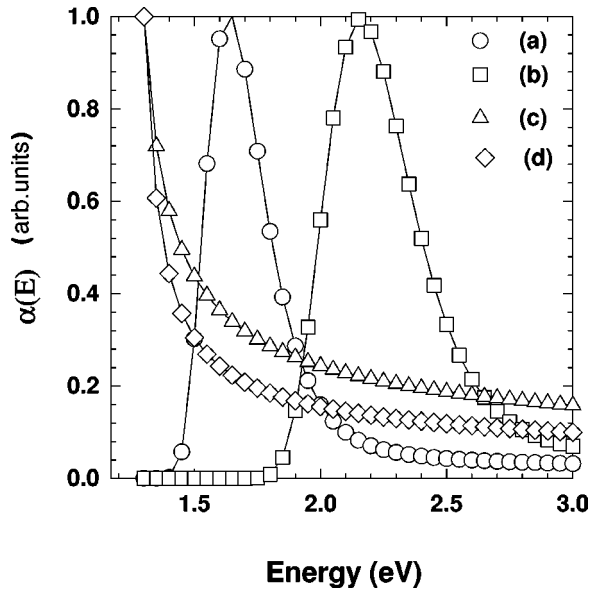


FIG. 5. Simulated $\alpha(E)$ vs E plot for direct transitions ($\gamma = 0$). Plots (a) and (b) are for cases (1) and (3) in Table I. Plots (c) and (d) are for cases (5) and (7) in Table I.

(cases 1 and 3 and cases 5 and 7 in Table I). To facilitate comparison between various cases, we have normalized the absorption to its peak value in each case. We see from the figure that the absorption tends to fall off at high energy (in sharp contrast with the experimental data). These results of the simulation can be easily understood as follows.

For a 1D system, the JDOS has a singularity at $E = E_G$ and falls off for $E > E_G$. The dominant contribution [to each $\alpha(E)$] is hence only from a particular set of nanostructures with band gap E_G , where $E = E_G$ and all other E_G 's have almost no contribution. So the simulated $\alpha(E)$ vs E plot mimics $P(E_G)$. We hence conclude from the simulation and the experimental data that PS is not a direct band-gap material and we will not consider this case further.

B. Indirect band gap

We now consider the case when momentum (k) is not conserved for the optical transition. Here we discuss two cases—size-independent oscillator strengths ($\gamma = 0$) and size-dependent oscillator strengths (assuming $\gamma = 6$).

We first consider the situation where the oscillator strength has no size dependence. Figure 6 [curves (a) and (c)] is a plot of the calculated α vs $\hbar\omega$ for a Gaussian distribution of sizes (cases 2 and 4 of Table I). Figure 7 [curves (a) and (c)] is a plot of the calculated α vs $\hbar\omega$ for a lognormal distribution of sizes (cases 6 and 8 of Table I). Also shown in the figures is a plot of the experimental curve for a p -type PS. (The dip in α near 2.2 eV in the experimental curve is an artifact related to a filter change.) To facilitate comparison, the calculated α is scaled to match the experimental curve near 3 eV. We see from the plots 6(a) and 6(c) that α initially increases with energy and then saturates—at variance with the experimental results. We understand this result qualitatively as follows. In Sec. I, we have already mentioned that the JDOS is a constant independent of energy for $\hbar\omega > E_G$ and zero for $\hbar\omega < E_G$. Hence for $\hbar\omega > E_G$, a given nanostructure contributes equally at all energies to α .

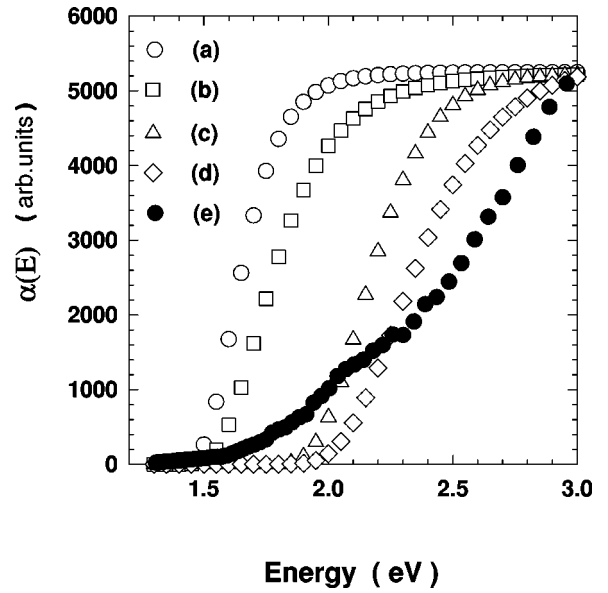


FIG. 6. Simulated $\alpha(E)$ vs E plot for indirect transitions. (a) and (b) correspond to case (2) in Table I for $\gamma = 0$ and 6, respectively. (c) and (d) correspond to case (4) in Table I for $\gamma = 0$ and 6, respectively. (e) Measured $\alpha(E)$ vs E plot for p -type PS.

However, $P(E_G)$ falls off as E_G increases. Nanostructures having a band gap (E_G) above a certain cutoff in energy (in the high-energy tail of the distribution) do not contribute significantly to $\alpha(\hbar\omega)$ [as $P(E_G)$ is very small]. This gives rise to the saturation of $\alpha(E)$ in Figs. 6(a) and 6(c). This saturation is more obvious in Figs. 7(a) and 7(c) because $P(E_G)$ falls off very rapidly for a lognormal distribution of sizes. These results also do not agree with the experimental data.

The situation is not remedied even if we include higher excited states ($n_x = 2$, $n_y = 1$, etc.) in the energy range considered in our calculation. Based on the above discussion, we

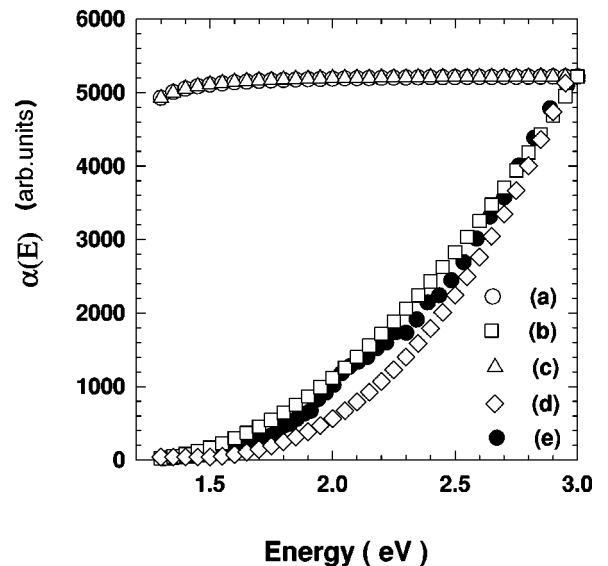


FIG. 7. Simulated $\alpha(E)$ vs E plot for indirect transitions. (a) and (b) correspond to case (6) in Table I for $\gamma = 0$ and 6, respectively. (c) and (d) correspond to case (8) in Table I for $\gamma = 0$ and 6, respectively. (e) Measured $\alpha(E)$ vs E plot for p -type PS.

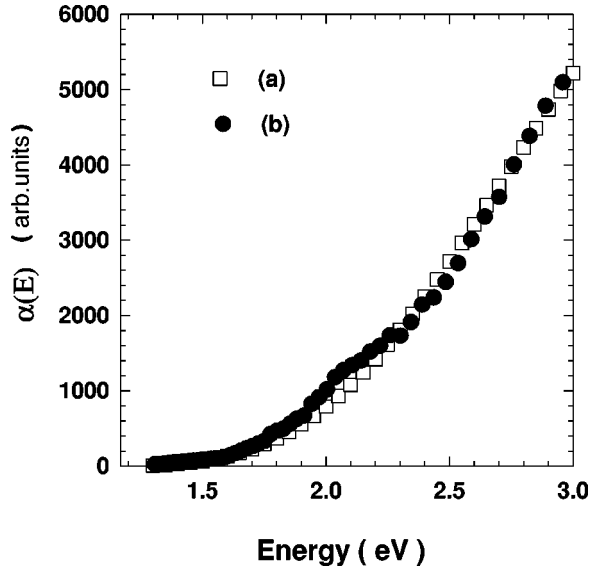


FIG. 8. (a) Simulated $\alpha(E)$ vs E plot for broad Gaussian distribution of band gaps ($E_0=2.25$ eV and $\sigma_E=0.75$ eV) with indirect transitions, $X=1.4$ and $\gamma=6$. (b) Measured $\alpha(E)$ vs E plot for *p*-type PS.

see that for α to increase with $\hbar\omega$, it is necessary to increase the contribution to α from the nanostructures in the high-energy region of $\alpha(E)$. This is possible if the oscillator strength is enhanced for the nanostructures with large E_G (smaller sizes).

We now consider the case when $F(E_G)$ varies as f/d^γ . Figure 6 [curves (b) and (d) for cases 2 and 4 in Table I] and Fig. 7 [curves (b) and (d) for cases 6 and 8 Table I] are plots of $\alpha(\hbar\omega)$ vs $\hbar\omega$ for $\gamma=6$. For the Gaussian distribution that we have chosen, we see that the absorption still saturates although the onset of saturation moves to slightly higher energy. This is a measure of the contribution of the (high energy) tail of $P(E_G)$ for the Gaussian case to the total absorption. For the lognormal distribution, we see from Fig. 7 [curves (b) and (d)] that $\alpha(\hbar\omega)$ vs $\hbar\omega$ now qualitatively looks like the experimental curve.

From a comparison of Fig. 6 and 7, we find that in order to get the absorption coefficient to increase with incident energy, it is important that the contributions to α from the low-energy regions of $P(E_G)$ do not dominate the optical absorption at large $\hbar\omega$. This is also satisfied if the distribution of band gaps $P(E_G)$ is sufficiently broad. We illustrate this in Fig. 8 where we plot the calculated value for α for a Gaussian distribution of band gaps with the mean energy at 2.25 eV and a variance of 0.75 eV. Hence we find that the nature of the band-gap distribution $P(E_G)$ plays a crucial role in determining the shape of the absorption spectrum.

We conclude that to properly account for the optical absorption in PS we need to assume (1) PS is a pseudo-1D indirect band-gap semiconductor; (2) the oscillator strength is size dependent and is given by a power law f/d^γ ; (3) the distribution $P(E_G)$ also plays an important role. Lognormal distribution of the nanostructures diameters in porous silicon seems to naturally account for the absorption spectrum.

All these considerations are in general agreement with the results of luminescence experiments on PS. The low-

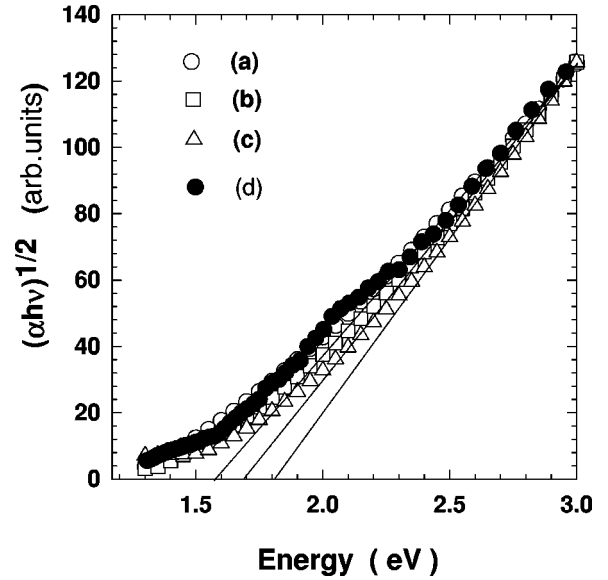


FIG. 9. Simulated plots of $(\alpha\hbar\omega)^{1/2}$ vs $\hbar\omega$ for (a) $\gamma=5$, (b) $\gamma=5.5$, (c) $\gamma=6.0$, and (d) corresponding plot for the experimental data on *p*-type PS.

temperature luminescence of PS excited near the peak of the broad luminescence spectrum exhibits steps which have been associated with the characteristic TO mode of *c*-silicon.²⁵ More recently²⁰ well-resolved peaks corresponding to the TO mode of Si have been reported for luminescence of PS, suggesting that PS is an indirect band-gap semiconductor. The observed dominant zero phonon component of luminescence constitutes direct evidence for the enhancement of the oscillator strength due to strong quantum confinement at smaller sizes.

We now comment on the validity of the procedure for obtaining the band gap of PS from $\sqrt{\alpha\hbar\omega}$ vs $\hbar\omega$. Figure 9 is a simulated plot of $\sqrt{\alpha\hbar\omega}$ vs $\hbar\omega$ (case 8 in Table I) for three different values of γ and the experimental data on *p*-type samples. First, we note that the intercept of the linear portion of each of the simulated curves is neither coincident with the peak position (near 1.3 eV) of the corresponding band-gap distribution (see Figure 4) nor close to the mean band-gap energy $E_0=2.25$ eV. So we see that it is very difficult to relate this intercept with such physical quantities. Therefore, it is not obvious how to interpret the intercept with some kind “effective band gap.” We also note that the intercept depends on the choice of γ . We hence believe that the intercept does not have the simple interpretation of a band gap as defined for a homogeneous system. We would like to point out that for such a heterogeneous system the gap can be interpreted only in an operational sense like E_{03} or E_{04} (the energy at which $\alpha=10^3$ and 10^4 cm⁻¹, respectively) depending on the value of the absorption coefficient (after correcting for the sample porosity).

Finally we try to understand the temperature dependence of the band gap. To explain the rigid shift of the absorption curve with temperature (to lower α), we argue that E_G of each of the nanostructures follows a relation $E_G(T)=E_{G0}-\gamma T$, where E_{G0} is the band gap at zero degrees Kelvin. We assume that the change of the band gap with temperature is a

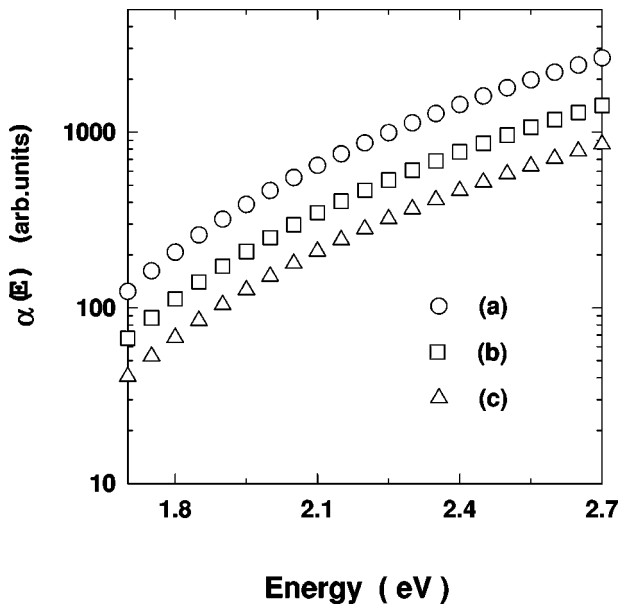


FIG. 10. Simulated $\alpha(E)$ vs E plots for various temperatures (for case 8 with $\gamma=6$). (a) $C=126=C_0$, (b) $C=1.25C_0$, (c) $C=1.5C_0$. Curves are rigidly shifted vertically from one another.

consequence, like in bulk semiconductors, of the electron-phonon interaction and take $\gamma=0.5$ meV/K. In our model, changing temperature is equivalent to changing the value of C in the expression that determines the energy upshift ΔE . Figure 10 is a plot of α vs $\hbar\omega$ for three different values of C . We see that the absorption curves are rigidly shifted vertically with respect to each other¹⁰ as also seen in Fig. 2. We argue that this provides a natural explanation for the observed temperature dependence of α .

V. CONCLUSIONS

In this paper we have investigated and clarified the absorption process in free-standing thin films of PS. We have elaborately discussed that one cannot use Eq. (1) to obtain the band gap of porous silicon. We point out that these objections are also true for other low-dimensional nanostructures like quantum wires, quantum dots, etc. One can easily generalize our results [Eqs. (8), (14), (15)] and use them to analyze the absorption process for other nanostructured materials too. For that purpose one just has to put the appropriate density of states function and the size distribution in those equations.

We have calculated the absorption coefficient as a function of energy assuming that PS can be modeled as a pseudo-1D system having a distribution of band gaps. From our calculations, we show that it is necessary to look at PS as an indirect band-gap material. To satisfactorily account for the absorption, we need to invoke that the oscillator strengths has a size dependence. We also show that a lognormal distribution of diameters of the nanostructures that make up PS appears to account for the measured absorption spectrum of p PS. We can explain the temperature dependence of the absorption in PS on the basis of our model, too. We have also shown that porosity can be inferred nondestructively from a transmission measurement in the region of low absorption.

ACKNOWLEDGMENTS

The authors would like to thank Professor B. M. Arora and Professor K. Rustagi for valuable suggestions. S.D. thanks Sandip Ghosh, Anver Aziz, M. K. Rabinal, and Biswajit Karmakar for useful discussions, and A. D. Deorukhkar, R. B. Driver, V. M. Upalekar, P. B. Joshi, and Subham Majumdar for their help.

*Electronic address: shouvik@tifr.res.in

¹L. T. Canham, Appl. Phys. Lett. **57**, 1046 (1990).

²A. G. Cullis and L. T. Canham, Nature (London) **353**, 335 (1991).

³V. Lehmann and U. Gosele, Appl. Phys. Lett. **58**, 856 (1991).

⁴Reuben T. Collins, Philippe M. Fauchet, and Michael A. Tischler, Phys. Today **50**(1), 24 (1997).

⁵Philippe M. Fauchet, in *Semiconductors and Semimetals*, edited by R. K. Willardson and E. R. Weber (Academic Press, Orlando, 1998), Vol. 49, p. 205.

⁶A. G. Cullis, L. T. Canham, and P. D. J. Calcott, J. Appl. Phys. **82**, 909 (1997).

⁷Yoshihiko Kanemitsu, Phys. Rep. **263**, 1 (1995).

⁸George C. John and Vijay A. Singh, Phys. Rep. **263**, 93 (1995).

⁹G. Bomchil, A. Halimaoui, I. Sagnes, P. A. Badoz, I. Berbezier, P. Perret, B. Lambert, G. Vincent, L. Garchery, and J. L. Regolini, Appl. Surf. Sci. **65/66**, 394 (1993).

¹⁰D. Kovalev, G. Polisski, M. Ben-Chorin, J. Diener, and F. Koch, J. Appl. Phys. **80**, 5978 (1996).

¹¹I. Sagnes, A. Halimaoui, G. Vincent, and P. A. Badoz, Appl. Phys. Lett. **62**, 1155 (1993).

¹²A. Kux and M. Ben-Chorin, Phys. Rev. B **51**, 17 535 (1995).

¹³Y. H. Xie, M. S. Hybertsen, William L. Wilson, S. A. Ipri, G. E. Carver, W. L. Brown, E. Dons, B. E. Weir, A. R. Kortan, G. P.

Watson, and A. J. Liddle, Phys. Rev. B **49**, 5386 (1994).

¹⁴J. I. Pancove, *Optical Processes in Semiconductors* (Prentice-Hall, Englewood Cliffs, N.J., 1971), Chap. 3.

¹⁵Sarah H. Tolbert, Amy B. Herhold, Christopher S. Johnson, and A. P. Alivisatos, Phys. Rev. Lett. **73**, 3266 (1994).

¹⁶J. von Behren, T. van Buuren, M. Zacharias, E. H. Chimowitz, and P. M. Fauchet, Solid State Commun. **105**, 317 (1998).

¹⁷Mark S. Hybertsen, Phys. Rev. Lett. **72**, 1514 (1994).

¹⁸G. D. Sanders and Yia-Chung Chang, Phys. Rev. B **45**, 9202 (1992).

¹⁹J. B. Khurgin, E. W. Forsythe, G. S. Tompa, B. A. Khan, Appl. Phys. Lett. **69**, 1241 (1996).

²⁰D. Kovalev, H. Heckler, M. Ben-Chorin, G. Polisski, M. Schwartzkopff, and F. Koch, Phys. Rev. Lett. **81**, 2803 (1998).

²¹H. Cramer, *Mathematical Methods of Statistics* (Princeton University Press, Princeton, 1946), Chap. 17.

²²A. J. Read, R. J. Needs, K. J. Nash, L. T. Canham, P. D. J. Calcott, and A. Qteish, Phys. Rev. Lett. **69**, 1232 (1992).

²³C. Delerue, G. Allan, and M. Lannoo, Phys. Rev. B **48**, 11 024 (1993).

²⁴V. Ranjan, Vijay A. Singh, and George C. John, Phys. Rev. B **58**, 1158 (1998).

²⁵P. D. J. Calcott, K. J. Nash, L. T. Canham, M. J. Kane, and D. Brumhead, J. Phys.: Condens. Matter **5**, L91 (1993).